Revision to: *Langmuir*
Date: March 24, 2016

Role of Side-chains in β-sheet Self-Assembly into Peptide Fibrils.

IR and VCD Spectroscopic Studies of Glutamic Acid-Containing Peptides

Fernando Tobias and Timothy A. Keiderling*

Department of Chemistry, University of Illinois at Chicago,

845 W. Taylor Street (m/c111), Chicago, IL 60607-7061 USA

Received: 00/00/00

* To whom correspondence should be addressed: tak@uic.edu, FAX: (312) 996-0431

Running Title: Impact of side-chain on β-fibril packing

ABSTRACT

Polyglutamic acid at low pH self-assembles after incubation at higher temperature into fibrils composed of antiparallel sheets that are stacked in a β_2-type structure whose amide carbonyls have bifurcated H-bonds involving the side chains from the next sheet. Oligomers of Glu can also form such structures, and isotope labeling has provided insight into their out-of-register antiparallel structure (Biomacromol. **2013**, *14*, 3880–3891). In this paper we report IR and VCD spectra and transmission electron micrograph (TEM) images for a series of alternately sequenced oligomers, Lys-(Aaa-Glu)$_5$-Lys-NH$_2$, where Aaa was varied over a variety of polar, aliphatic, or aromatic residues. Their spectral and TEM data show that these oligopeptides self-assemble into different structures, both local and morphological, that are dependent on both the nature of the Aaa sidechains and growth conditions employed. Such alternate peptides substituted with small or polar residues, Ala and Thr, do not yield fibrils; but with β-branched aliphatic residues, Val and Ile, that could potentially pack with Glu side chains, these oligopeptides do show evidence of β_2-stacking. By contrast, for Leu, with longer sidechains, only β_1-stacking is seen while with even larger Phe side chains, either β-form can be detected separately, depending on preparation conditions. These structures are dependent on high temperature incubation after reducing the pH and in some cases after sonication of initial fibril forms and reincubation. Some of these fibrillar peptides, but not all, show enhanced VCD, which can offer evidence for formation of long, multistrand, often twisted structures. Substitution of Glu with residues having selected side chains yields a variety of morphologies, leading to both β_1 and β_2 structures, that overall suggests two different packing modes for the hydrophobic sidechains depending on size and type.

INTRODUCTION

Numerous studies in recent years have addressed protein misfolding and self-assembly that can result in very stable, β-sheet-rich fibril structures. These are of particular mechanistic interest for several biomedical applications, since amyloid fibrils are symptomic of neurodegenerative diseases such as Alzheimer's, Huntington's, Creutzfeldt-Jakob and other prion diseases.[1–4] Such self-assembled structures are of added interest in materials science due to the potentially tunable nature of their β-sheet rich scaffold, which could also have pharmaceutical applications.[5,6]

A wide variety of proteins and peptides can be induced to form fibril structures, depending on external conditions such as pH, ionic strength, temperature, concentration.[7] A common driving force in this process is the aggregation of hydrophobic parts of the molecules and formation of sheet structures that can reassemble into extended and more ordered forms. Several studies have shown that the sheet structures can pack one above the other in different morphologies by interleaving sidechains arising from residues in oppositely facing β-sheet segments.[8–12] Direct evidence of this interleaving structure can be seen in the infrared (IR) spectra of synthetic polyglutamic acid (PLGA) samples, that are prepared at relatively low pH and incubated at elevated temperatures, under which conditions they develop the so-called β_2-sheet form.[13–16] The amide carbonyls in these structures participate in bifurcated H-bonds both in the normal way, i.e. to N-H groups on the neighboring strand within each sheet, and additionally to –COOH groups associated with Glu side-chains in the next sheet lying above or below along a stack of sheets. By use of a sequence of Glu residues one gains a convenient probe of sheet-sheet interaction, whose self-assembly is mediated by interleaving of the sidechains. Simple detection of this higher level of structure would not be possible with other types of residues, for example, the widely studied polyglutamine peptides, which are models for the fibrillar state involved in Huntington's disease.[17,18] Use of low pH Glu provides a detection scheme for self-assembly of

densely packed side chains in a structure that has parallels in other assemblies of biological or materials interest.

Normal anti-parallel β-sheets have amide I (primarily C=O stretch) IR spectra dominated by a sharp band at ~1615-1625 cm^{-1} with a weak band at ~1680-90 cm^{-1},[19–21] which has been termed the β_1 form. In the Raman a single band dominates, that lies between these two extrema, often at ~1660-70 cm^{-1}. This overall frequency spread between amide I components, and the commonly used frequency shift of the IR maximum from those of helical and disordered structures, is due to exciton coupling and not to H-bonding strengths. The coupling between local amides, as influenced by the stereochemistry or repeat secondary structure geometry, results in an intensity dispersion that develops a characteristic band position and is thus diagnostic of conformation. If the sheet is small or distorted, such as typical in a globular protein, the spectra are broader, and the lower frequency component is higher, 1630-40 cm^{-1}. Self-assembly of sheets into the β_2 form is characterized experimentally in the IR by a down-shifted amide I band whose dominant intensity maximum lies below 1600 cm^{-1} and has a significant shoulder at ~1640 cm^{-1}. This 1640 cm^{-1} band in the β_2 form is not a shifted upper exciton component seen in the β_1 structure, but rather overlaps the dominant amide I component that is experimentally seen in the Raman spectra of these PLGA or Glu_n fibrils (hence this band is termed the Raman-allowed amide I).[14,15] Thus the main amide I bands in both the Raman and IR are dramatically shifted down (>20 cm^{-1}) indicating a change in the diagonal force field (FF), which has been ascribed to added, bifurcated H-bonding to –COOH groups on the protonated Glu side chain of an opposing, stacked sheet.[14] However, the expected, weak, higher frequency exciton-split component of the amide I (normally ~1680-90 cm^{-1} for anti-parallel sheets) is not evident in the β_2 form. The original observation of β_2 formation in PLGA showed that these IR trends correlated with fibril

aggregates having a more compact structure, as indicated by x-ray diffraction lines corresponding to an ~8 Å layer separation, as opposed to the more expanded ~9 Å spacing found for PLGA β_1 structures (which would also be typical for other β-sheet forming polypeptides, such as polyLys at high pH).[13,19,22] These variances in separation correspond to the sheet packing dimension, but both forms have the normal cross-strand H-bonded repeat distance between strands in the antiparallel sheets. Such insoluble fibrillar structures are difficult to characterize with conventional biophysical methods, so that existing structural evidence is often based on fiber diffraction and electron microscopy, as well as infrared (IR) and Raman or solid-state NMR spectroscopic results.[23–25]

Lowering the pH of oligoGlu converts the oligomer from a charged to a neutral species, thus eliminating charge repulsion between side chains and sharply increasing their hydrophobicity, which leads to aggregation, particularly when heated. [Without heating, polyGlu at low pH forms a partially helical structure.[26–30]] While very low pH values may not be biologically important, it provides a clear means of detection of interleaving of neutral side chains in a highly compact stacked sheet structure. Such hydrophobicity can of course be attained by oligomers of residues with apolar side chains, but for such cases the β_2 formation diagnostic is lost, so low pH Glu offers a unique detection scheme for compact side-chain packing in fibrillar or β-sheet containing states. To study the impact of exchanging various other residues for Glu on this self-assembly process, we have constructed a series of oligomers with a common sequential form of Lys(Aaa-Glu)$_5$Lys-NH_2 where Aaa is an uncharged residue, polar or nonpolar (sequences and notations are shown in Table 1). For our purposes (ease of purification) we terminated the oligomers with Lys to enhance solubility, resulting in a series of dodecapeptides. The same sequence with Aaa = Glu was prepared as a control. IR and

vibrational circular dichroism (VCD) spectroscopic studies were carried out and correlated to transmission electron micrograph (TEM) images of the fibril deposits. The formation of partially

Table 1. Notation and sequences of Lys(Aaa-Glu)$_5$Lys peptides

Aaa	Notation	Sequence	Side chain branching
Glu	$(E)_{10}$	KEEEEEEEEEEK-NH_2	polar, charged
Ala	$K(AE)_5K$	KAEAEAEAEAEK-NH_2	nonpolar
Thr	$K(TE)_5K$	KTETETETETEK-NH_2	polar, uncharged
Val	$K(VE)_5K$	KVEVEVEVEVEK-NH_2	β-branched, nonpolar
Ile	$K(IE)_5K$	KIEIEIEIEIEK-NH_2	β-branched, nonpolar
Leu	$K(LE)_5K$	KLELELELELEK-NH_2	γ-branched, nonpolar
Phe	$K(FE)_5K$	KFEFEFEFEFEK-NH_2	γ-branched, nonpolar

β_2-form sheets was shown to depend on the characteristics of the side chain, and the preparation conditions used. The morphological character varied with side chain as well.

EXPERIMENTAL SECTION

Peptide Synthesis and Purification

Peptides were manually synthesized using standard fmoc chemistry with blocked amino acids obtained from Anaspec, Inc. Each peptide was synthesized on a 0.1 mmol scale. Rink amide resin from Anaspec, Inc. was used as the solid support to provide C-terminal amidation.[31,32] HPLC purification was done with a Vydac 218TP510 C-18 reversed-phase column on a Waters 600 system using an acetonitrile (ACN) solvent gradient from 20% ACN/80% H_2O to 85% ACN/15% H_2O both with 0.1 % trifluoroacetic acid (TFA). Mass

verification was done by electrospray ionization mass spectrometry (ESI-MS) at the UIC Research Resources Center (RRC).

Sample Preparation

For Transmission IR (FT-IR) and VCD, solutions were made by suspending peptide samples in D_2O and adjusting to pD ~2 with deuterated hydrochloric acid (DCl). Initial spectral measurements were made on freshly made samples, which were followed by measurements on incubated samples. For the latter, peptide solutions were sonicated and aliquoted into another Eppendorf tube, sealed with parafilm to prevent evaporation, and incubated for 48 hours at 65°C or 75°C.

FT-IR/ VCD

Transmission Fourier Transform IR (FT-IR) spectra were measured at 4 cm^{-1} resolution as an average of 512 scans using a Bruker Vertex 80 spectrometer with a DTGS detector, and then were baseline subtracted with a spectrum of D_2O and normalized to a constant absorbance area in the amide I region. All the peptides were deuterium exchanged and lyophilized at pH <1 to remove residual trifluoroacetic acid (TFA) used in synthesis and purification. Peptide samples for IR and VCD studies were dissolved in D_2O and adjusted to pD 2 and to a final concentration in the range of 10 - 25 mg/mL and were studied either fresh or after incubation by placing them in our usual homemade transmission cells[33] constructed from two CaF_2 windows separated by a 50 μm Teflon spacer and mounted in a brass holder.

VCD experiments were carried out using a homemade dispersive instrument that has been previously described in detail.[34] The same samples made for FT-IR were measured for VCD. The spectra were obtained as an average of four to six repeated scans and measured over the 1800 to 1500 cm^{-1} region. Scans of D_2O solvent in an identical cell were obtained as

baselines using the same conditions as the sample and were subtracted from the sample spectra. Film and fibrillar samples are prone to polarization artifacts, and the dispersive VCD can in some cases be optically aligned more easily to minimize these than FT-VCD. [33,35] To detect any potential problems due to sample orientation effects, the VCD spectra were measured over successive sample rotation angles to assure we were comparing spectra from isotropic responses. Unfortunately our instrument is not yet equipped with the dual modulator modification designed by Nafie that might further minimize this problem.[36]

Transmission Electron Microscopy

Transmission electron microscopy (TEM) images were taken in the UIC-RRC with a JEM 1220 electron microscope (JEOL Co. Japan), operated at 80 kV with a Gatan Es1000W 11MP CCD camera. Selected samples were also run at higher voltages (300 or 200 kV) for improved contrast with a JEOL JEM-3010 instrument. Samples consisted of 15 μL of suspended precipitate peptide prepared at 0.1 wt % in H_2O, applied to copper grids (400 mesh) coated with carbon (Electron Microscopy Science) for 1 min, blotted with filter paper, negatively stained for 45 s with 2 wt % uranyl acetate and then dried at room temperature.

RESULTS

Effect of the terminal lysines on $KGlu_{10}K$ fibril formation

To study the effect of different side chains on β_2 fibril formation with alternating $(Aaa\text{-}Glu)_5$ peptides, it is important to first assess the effect of adding lysine to the C and N-termini for solubility enhancement. As a control, we prepared the corresponding $KE_{10}K\text{-}NH_2$ peptide and demonstrated that fibril formation both is possible after this modification and gives results consistent with those of our previous Glu_{10} oligomer studies.[31] Most of the amino acids studied

here as substitutes for Glu in these oligomers are hydrophobic, and addition of lysine was crucial to obtain adequate solubility for low pH HPLC peptide purification (resulting from TFA addition), which neutralizes (protonates) the Glu side-chains that have a nominal pK_a of 4.15, but Lys remains charged. Low pH is needed for these fibril studies because the uncharged side-chains can then participate in the three-centered hydrogen bond formation that this study uses as a structure diagnostic. Finally the Lys additions should lead to the peptides initially forming sheets whose strands are in register, enhancing order in the final self-assembled (stacked) structures.

After dissolving in D_2O and adjusting to pD ~2, FT-IR and VCD spectra of $KE_{10}K$ were obtained (Figure 1). The FT-IR spectrum after incubation at 75-85 °C (Figure 1C) closely resembles that obtained in our previous study for E_{10} at pH ~1 (i.e. without lysine termination). The amide I' region for the sample has a low frequency peak at 1594 cm^{-1} characteristic of β_2 sheet formation with a weaker band at ~1639 cm^{-1}. As compared to the freshly prepared sample, the amide I' features sharpen and the shoulder in the fresh sample IR spectrum at 1604 cm^{-1} disappears after high temperature incubation. The characteristic double peaks at 1730 and 1720 cm^{-1} assigned to stretching vibrations of the carboxylic acid C=O in the protonated Glu side chains can be clearly seen in the spectra for both samples. However, the weak, mostly negative VCD (Figure 1A) for the freshly prepared sample implies that its sheet segments have not yet self-assembled into extended fibrils. TEM results (Figure S1, Supporting Information, SI) support this, showing that only shorter, poorly developed fiber segments and small aggregates were evident in the freshly prepared $KE_{10}K$ samples. This is in contrast to data for the previously studied Glu_{10} oligopeptides, which spontaneously formed extended, twisted structures with multiple fibrils clustering at low pD.[31] However, after incubation at high temperature for 48

hours, $KE_{10}K$ self-assembled into a β_2-type fibril structure, evident for the IR (Fig. 1 C), which additionally exhibited an enhanced amide I' VCD couplet centered at 1590 cm^{-1} and a substantial couplet at ~1720-30 cm^{-1} (Figure 1B). These match the band shapes of previously published results for PLGA and Glu_{10}, i.e. sequences without terminal Lys residues. TEM images (Figure S1, SI) of mature $KE_{10}K$ fibrils show long, relatively thin fibers that under higher magnification and contrast appear to be flat ribbons that tend to pair side-to-side and slowly twist over a longer length scale, the observation of which complements the enhanced VCD intensity.

$(Ala\text{-}Glu)_5$ and $(Thr\text{-}Glu)_5$

Alanine and threonine-substituted oligomers, $Lys(Ala\text{-}Glu)_5Lys\text{-}NH_2$ and $Lys(Thr\text{-}Glu)_5Lys\text{-}NH_2$, were synthesized to provide a set of reference data with sequences where Glu is substituted with small or polar residues in contrast to peptides where Glu is substituted with larger and more hydrophobic side chains (following sections). For these two alternate peptides, the substituted (Aaa) side chain does not enhance fibril formation and provides a potential monitor of the effect of side chain polarity on the peptide structure and fibril morphology. FT-IR and VCD spectra were measured for freshly dissolved samples in acidic conditions, and these exhibited spectra characteristic of a disordered or statistical coil conformation[37] (or, as has been extensively established, one that has local inter-residue coupling matching that of PPII)[38,39] (Figure 2). Even after high temperature incubation for 48 hours, only minor spectral changes were observed for these two variants. Both samples evidenced spectra dominated by a broad amide I' absorbance centered around 1650 cm^{-1} and a relatively weak negative VCD couplet (negative-to-positive, from low to high frequency), consistent with a locally PPII-like conformation, see Figure 2 and Figure S2 SI, respectively, for $K(AE)_5K$ and $K(TE)_5K$ spectra. (Weak features to lower frequency may suggest a small degree of initial aggregation.) The

corresponding TEM images (Figure S3, SI) show only small aggregate particles that did not mature into fibrils, even after incubation at 85 °C.

$(Ile\text{-}Glu)_5$ and $(Val\text{-}Glu)_5$

Isoleucine and valine, when substituted into the alternating Glu oligomer sequences, resulted in peptides with spectra that exhibited a contrasting behavior from the above peptides. At low pD, these alternate peptide models exhibited similar secondary structures as seen by their FT-IR (Figure 3B, $K(IE)_5K$, and Figure S4, SI, $K(VE)_5K$). As for the $KE_{10}K$ sequence, both these β-branched aliphatic side chain peptide sequence variants, containing Ile or (Val), immediately adopted the β_2 form as seen from their 1605 (1602) cm^{-1} main amide I' peak plus the appearance in the IR of the 1658 (1650) cm^{-1} Raman-allowed peak and the enhanced intensity and shift of the sidechain carbonyl stretching mode up to 1730 cm^{-1}. High temperature incubation slightly further developed the β_2 sheet structure, as indicated by the modest attenuation of the 1620 cm^{-1} peak which corresponds to the normal β_1 cross-strand H-bonded amides. Since these sequences include only half Glu residues, half the amides must have only normal single cross-strand H-bonds, consequently this β_1-like IR feature must persist, even in a well-formed β_2-sheet structure. The peak at 1730 cm^{-1}, which is assigned to the C=O of the Glu side-chain -COOHs, appeared as a single peak, much as was seen previously for the isotopically-substituted E_{10}-like oligomer sequences containing one or two Val residues.[31]

Despite clear formation of β_2 structure, VCD spectra of these peptides did not show any significant intensity enhancement even after incubation (Figure 3A), but samples of the $K(VE)_5K$ peptide showed a VCD orientation dependence under these sample preparation conditions. Consequently VCD data for $K(VE)_5K$ are not shown, since it is not possible to obtain structural information from such spectra. These orientation phenomena indicate some type of self-assembly

into locally ordered domains in the sample. (For a fibrillated sample, this would imply side-to-side organization of the macrostructures.) The VCD enhancement tends to correlate with fibril formation, but it is not a necessary result of fibrilization. The strongest VCD enhancements tend to be associated with twisted and multiple strand fibrils.[40–42] TEM images for $K(VE)_5K$ and $K(IE)_5K$ (Figure S5, SI) do indicate formation of twisted fibrils, but they are relatively short, which may be one reason for their very weak VCD intensity (Figure 3A). The TEM images show similar morphologies for both peptides; appearing as short rod-like aggregates that assemble into larger clusters. Even after incubation, there were no significant differences, but the $K(VE)_5K$ sample images showed larger flat local clusters that had fibrils aligned side-to-side, which may be one source of their VCD orientation dependence (Figure S5A, SI).

$(Leu\text{-}Glu)_5$

By contrast, FT-IR spectra of freshly prepared $K(LE)_5K$ indicated formation of a β_1 sheet conformation as evidenced by the sharp peak at 1616 cm^{-1} and high frequency component at 1685 cm^{-1} (Figure 4C). It can be noted that this is the characteristic vibrational mode frequency dispersion (exciton splitting) found for many peptide-based amyloid fibril structures, particularly those that are essentially forming antiparallel sheets.[43–45] This is the only $(Aaa\text{-}Glu)_5$ variant studied that formed a well-defined β_1 sheet structure immediately upon exposure to acidic pD and maintained it after incubation. However, the VCD of the freshly prepared sample corresponding to this FT-IR showed an orientation dependence that underwent full sign reversal on rotation of the sample through 180° (Figure 4A). When this sample was subjected to ultrasonication and then incubated at high temperature, the orientation dependence of the VCD was dramatically reduced, having just a minor residual intensity variation, which could be due to some sample inhomogeneity (Figure 4B). Multiple sample preparation attempts had varying

success in removing the orientation dependence of the VCD intensity, although a consistent sign pattern could be obtained. Extended or aggregated fibril formation was suggested by the significant VCD enhancement after incubation (compare Figures 5 A, B), yet the secondary structure of the stacked sheets remained in the β_1 form, with little change in IR and no significant VCD for the Glu side chain –COOH mode (Figure 4C). These enhanced amide I' VCD intensities correlate with TEM images which show a network of long fibers that appear to be twisted pairs of strands, but these fibrils are independent of β_2 structure formation (Figure S6, SI). Some $K(LE)_5K$ samples showed residual VCD intensity orientation dependence but had clusters of many shorter fibrils, evidencing less successful fiber growth even though they had a gel like consistency (Figure S6, SI, right).

$(Phe\text{-}Glu)_5$

Aromatic residues such as phenylalanine have been found in many amyloidogenic peptides like β-amyloid and can further stabilize sheet formation by means of π–π interaction of the aromatic side chains.[46–48] At pD 2, FT-IR spectra of $K(FE)_5K$ show this peptide initially adopted a characteristic β_1-sheet structure as evidenced by the sharp peak at 1621 cm^{-1} and a weak feature at 1686 cm^{-1} (Figure 5C). The VCD of the initially formed sample had only modest intensity, but exhibited an orientation dependence (Figure 5A). This $K(FE)_5K$ sample was then sonicated and incubated at high temperature, much as for the $K(LE)_5K$ sample above, and the orientation dependence essentially disappeared while its FT-IR (Figure 5C) indicated a conversion from pure β_1 to a primarily β_2 form. This new form has two dominant amide I peaks since only the Glu side chains can form bifurcated H-bonds to the amides on the opposing sheet, resulting in the lower frequency band, but the amides opposite the Phe side chains cannot participate in bifurcated H-bonding, and thus still retain the 1620 cm^{-1} peak.

This sonication and reincubation step has been used in seeding experiments where preformed fibrils are introduced to solutions of non-aggregating peptides[14,49–51] and has been used to decrease fibril size variation and to favor sample homogeneity. In $K(LE)_5K$ as in most cases, the conformation was maintained. However, in the $K(FE)_5K$ case dramatic changes in the spectra are seen, with a sharp peak at 1601 cm^{-1} and another at 1650 cm^{-1} appearing in the amide I' FT-IR plus a shift of the –COOH feature to 1730 cm^{-1}, which are all indicative of the formation of β_2 sheets. Such a change in structure and overall morphological order that is stimulated by sonication and heating suggests that the initial β_1 form was the result of a kinetic trap and that the β_2 form is a lower energy structure. The unusual conformational transition for $K(FE)_5K$ was further evident in the enhancement of its VCD intensity (Figure 5B), whereby the peak-to-peak scale increased by about 60-fold. The couplet VCD perhaps surprisingly reflects both of these dominant amide I features, being positive at 1601 cm^{-1} and negative at 1625 cm^{-1}. As noted above, even if fully regular β_2 stacked sheets are formed, two kinds of amide I' bands must be present, one for amides H-bonded to a Glu side chain (1601 cm^{-1}), creating bifurcated hydrogen bonds, and the other normally just cross-strand H-bonded (1620 cm^{-1}), presumably those amides directed at or shielded by a phenylalanine side chain. This would be true if the β_2 stacking was such that the Phe and Glu side chains interleaved or if they instead alternately formed Glu-Glu and Phe-Phe interactions. However the latter situation is more probable given the steric interference the Phe side-chain would introduce if interleaved with Glu. The doubled amide I' peaks of $K(FE)_5K$ are also split somewhat farther apart (19 cm^{-1}) and better resolved as compared to those seen for $K(VE)_5K$ and $K(IE)_5K$ (18 cm^{-1} and 15 cm^{-1}, respectively), indicating $K(FE)_5K$ forms a more extended or better defined β-structure repeat.

The TEM images of the $K(FE)_5K$ samples show a difference in morphology that developed after high temperature incubation. The freshly prepared sample had a network of fibers with different strand widths (Figure 6A). Although long fibrils are present, twists cannot be distinguished. However, after incubation, more homogenous fibrils were seen with evident twisting as seen in Figure 6B. These apparent long twisted fibers are consistent with the sharply enhanced amide I'VCD intensities for the sonicated and incubated sample.

DISCUSSION

Many peptides and proteins aggregate when perturbed by pH change due to neutralization of charged residues which can either lead to unfolding or to structural rearrangement. This can provide a potential for aggregation due to an increase in the hydrophobicity of residues that would have been originally exposed to solvent. Many of these aggregation processes eventually lead to formation of long, relatively well-organized fibril structures with an underlying β-sheet structure, a structure change that often can be induced after incubation at higher temperatures, increase in concentration and/or change in ionic strength. In this study we focused on initiation of fibril formation by protonation, and hence neutralization, of glutamic acid and its consequences for short peptides of mixed, alternate sequences. The unique aspect of Glu residues in promoting aggregation is that at low pH the –COOH groups can provide H-bonding partners to the amide C=O groups from peptide chains in other segments of the overall packing structure. When the strands are arranged in a β-sheet conformation, this allows bifurcated H-bonding between two separate sheets resulting in formation of the stacked β_2-sheet structure. This added H-bonding shifts the characteristic amide I down in frequency (by ~20-30 cm^{-1}), and distorts the dipole moments so that the normally quite weak Raman allowed band can be seen in the IR

(albeit also shifted by a similar amount). This β_2 variant has a very compact layer structure and develops a unique spectral response that lets us monitor organized structure or fibril formation and intercalation of side chains on fibril formation. While this β_2-sheet conformation is well-known for longer chain polymers, recently it has been shown to be a valid model for oligomers as well.[13–15,31,52] Previous work suggested that not all residues needed to be Glu to enable β_2-structure formation and that hydroscopic residues were structure preserving.[13,31] We have demonstrated here that alternate $(Aaa\text{-}Glu)_5$ peptides can also form β_2-structures, although in this case they must exhibit two dominant low frequency bands since only half of the amide C=O groups can have bifurcated H-bonds. However our study develops new questions regarding what residues are consistent with such a structure and what kind of structure do they develop beyond the cross-strand H-bonding typical of a β-sheet secondary structure.

The $(Aaa\text{-}Glu)_5$ data presented here suggest that to form fibrils the alternate Aaa residues should be hydrophobic, since Ala and Thr both resulted in PPII-like or random coil structures. This may be a result of length,[52] but at least for decapeptides it seems consistent. Secondly the hydrophobic residues must be compatible to pack with Glu in some manner, for example, to interleave as seen in PLGA and Glu_{10}.[13,53] This same structure is not found in polyLys nor is it seen (in our hands) in polyAsp, so the side chain length and nature of the H-bond donor are important driving forces.[19–22] Our results show that when substituted in alternate sequence oligomers with Glu, Val and Ile with β-branched aliphatic sidechains led to formation of β_2 structures, while the γ-branched Leu yielded well-formed β_1 structures that did not convert to a β_2 structure even after high temperature incubation and sonication, typical perturbations used to disrupt or anneal trapped aggregate conformations. The β-branched examples studied both contribute to the hydrophobic packing in the sense that, due to branching, they provide some

shielding of the nearby amides from the solvent. Furthermore the side chains are shorter allowing them to make an easier fit between Glu sidechains, if both were interleaved. Alternatively if not interleaved with Glu, the Val or Ile side chains could be on the outside of a pair of sheets leading to a hydrophobic "sandwich" that, by stacking pairs of sheets with hydrophobic exterior surfaces, could still extend in the interstrand H-bonding direction. Such structures would have any extended stacking (beyond a pair of sheets) stabilized primarily by van der Waals interactions, which would presumably be less likely to result in multistrand fibers, especially with just aliphatic interactions, and less likely to develop enhanced VCD. This would fit what we have seen for Val and Ile. Leu, on the other hand, while similarly able to provide hydrophobic shielding of the backbone amides, is longer and has an isobutyl group terminating the chain, which might pose some packing problem and potentially shift the sheets apart, beyond H-bonding distance, if interleaved with Glu. If the interleaving of these branched hydrocarbon chains were stable, the size of Leu might inhibit development of bifurcated H-bonds and favor a β_1 structure and formation of extended stacked fibrils resulting in enhanced VCD.

Looking at just these aliphatic residues, the story would seem to be consistent, however the Phe result raises added questions. Clearly the Phe side chain is much larger than those for the aliphatic models studied and might provide a different kind of hydrophobic shielding/interaction. It seems unlikely that Phe would make a matching fit in the space between the Glu sidechains in a stack of sheets, and, if it did, even more unlikely that it could allow formation of the compact β_2 structure with the Glu side chains reaching to opposite amide groups. Upon fresh preparation at low pH, the $K(FE)_5K$ peptide forms a β_1 structure consistent with hydrophobic collapse and formation of cross strand H-bonds in a "normal" β_1-type sheet, which may or may not be stacked. The sharpness of the amide I bands argue for its forming an extended structure, though

not necessarily fibril formation, but the TEM confirms fiber containing structures are present for fresh samples, although they cluster and are thin.

However, after sonication and a second high temperature incubation, β_2 structures are formed, as clearly seen in the IR. These are quite organized and extended, as evidenced by the sharp IR features and the VCD enhancement. From the TEM results, the fibrils are clearly twisted and form long multistrand structures, which again are consistent with previous observations of conditions under which VCD intensity is markedly enhanced.[40–42] The result showing sharp IR spectra and enhanced VCD strongly suggests that one conformation or packing arrangement is dominant, again with the lower and higher frequency split dominant amide I' features being due to those amides with bifurcated and normal cross-strand H-bonding respectively. The VCD of a single couplet encompassing both these "split" amide I features suggests the normal and bifurcated H-bonded amide C=O groups couple to develop the observed spectra pattern. Such a conformational change suggests the interaction between β-sheets formed from the $K(FE)_5K$ oligomers may have become dual-layered or "sandwich-like" in nature, with the Glu side chains on the "inside" interacting sheet-to-sheet, forming stabilized sheet-sheet interactions via bifurcated H-bonds as found in PLGA, thereby leaving the Phe side chains on the "outside". While two interacting layers most likely make up the base structural component for the $K(FE)_5K$ fibrils after incubation, stacking of multiple dual layers is certainly possible. This fibril form has a second potential stabilization mechanism, in which the phenyls from the Phe side chains could have a π–π interaction, stacking or otherwise.[47,54,55] On incubation such a π-stacking interaction might provide a driving force for a structural rearrangement from β_1- to β_2-form. As a result, one would expect a sheet-to-sheet distance to be like that of polyGlu for the inside interaction, but a different layer distance for any stacking between the outside layers.

Unfortunately, our attempts to obtain x-ray diffraction data of sufficient quality to resolve this stacking structure have been unsuccessful.

VCD intensity enhancement has been proposed as a means of identifying fibril formation, or more particularly morphological discrimination among fibril types.[41,42,56] It is clear that the enhancement alone does not indicate fibrilization, as some fibril types give weak enhancement, particularly those forming thin and short fibrils. Twisted, multistrand fibrils seem to have the strongest VCD, as has been shown by Nafie and coworkers.[41] Use of VCD in this study provides an added observation for discriminating fibrilization morphologies. However, detection of β_2 forms by their amide I IR pattern is the prime method for discriminating stacking types and for detecting compact interleafed side chains. Combining these spectral data with TEM makes the structural analysis more complete.

CONCLUSION

Our studies show that alternate peptides of the form $(Aaa\text{-}Glu)_n$ can self-assemble into extended β-sheets and fibril forms even for decapeptides, provided that the Aaa residue is hydrophobic. The spectra show that β_2 formation is possible for β-branched aliphatic residues (Val and Ile) substituted in this sequence, but by contrast longer aliphatic side chains (Leu) resulted in β_1 formation. On the other hand, the Phe result was anomalous in that it led initially to β_1 formation and then was stabilized as β_2, depending on which preparation conditions were used. This change presumably resulted from one type of stacking being a kinetic trap which was overcome allowing access to what appears to be an energy minimum structure.

The pattern of agreement in spectral shape of the β_2 structures from the alternate peptides and those of $KE_{10}K$ suggest that all are antiparallel β-sheets.[31,57] This is expected as the

antiparallel form tends to dominate conformations found for short oligomers forming β-sheet structures, partly due to its more stable H-bond pattern. With the β_2 structure, the traditional FT-IR diagnostic for detecting such an antiparallel form is not useful, since the high frequency component is not seen. For these systems, the NMR approaches often used to determine structures in fibril systems may also not be effective due to the high degree of degeneracy in such alternate sequence peptides, which would inhibit assignment of unique resonances without specific site labeling.[58,59] However registry in those alternate peptides remains an issue that can most easily be determined by isotopic labeling and IR/VCD studies as we and others have previously demonstrated.[31,57,59–61] The behavior of these synthetic model peptides in forming aggregates and fibrils may offer insight into the fundamental mechanisms influencing such processes in amyloid diseases.

Acknowledgements

We thank Linda Suarez, Figen Seiler and Alan Nichols of the RRC-EMS Facility for assisting in obtaining the TEM images, Prof. Jordi Cabana and Mark Wolf of UIC for discussions of and efforts to obtain XRD for fibrils, Prof. Petr Bour and Jiri Kessler of the Academy of Science, Prague, for model fibril schematics, and Wojciech Dzwolak, Warsaw University, for discussions of the results.

References

(1) Chiti, F.; Dobson, C. Protein Misfolding, Functional Amyloid, and Human Disease. *Annu. Rev. Biochem.* **2006**, *75*, 333–366.

(2) Caughey, B.; Lansbury, P. T. Protofibrils, Pores, Fibrils, and Neurodegeneration: Separating the Responsible Protein Aggregates from the Innocent Bystanders. *Annu. Rev. Neurosci.* **2003**, *26*, 267–298.

(3) Dobson, C. Protein Folding and Misfolding. *Nature* **2003**, *426*, 884–890.

(4) Schnabel, J. Protein Folding: The Dark Side of Proteins. *Nature* **2010**, *464*, 828–829.

(5) Itoh, K.; Tokumi, S.; Kimura, T.; Nagase, A. Reinvestigation on the Buildup Mechanism of Alternate Multilayers Consisting of Poly(l-Glutamic Acid) and Poly(l-, D-, and Dl-Lysines). *Langmuir* **2008**, *24*, 13426–13433.

(6) Zhang, S. Lipid-like Self-Assembling Peptides. *Acc. Chem. Res.* **2012**, *45*, 2142–2150.

(7) Dobson, C. M. Protein Misfolding, Evolution and Disease. *Trends Biochem. Sci.* **1999**, *24*, 329–332.

(8) Nelson, R.; Sawaya, M. R.; Balbirnie, M.; Madsen, A. Ø.; Riekel, C.; Grothe, R.; Eisenberg, D. Structure of the Cross-Beta Spine of Amyloid-like Fibrils. *Nature* **2005**, *435*, 773–778.

(9) Tycko, R. Molecular Structure of Amyloid Fibrils: Insights from Solid-State NMR. *Q. Rev. Biophys.* **2006**, *39*, 1–55.

(10) Sawaya, M. R.; Sambashivan, S.; Nelson, R.; Ivanova, M. I.; Sievers, S. A.; Apostol, M. I.; Thompson, M. J.; Balbirnie, M.; Wiltzius, J. J. W.; McFarlane, H. T.; et al. Atomic Structures of Amyloid Cross-Beta Spines Reveal Varied Steric Zippers. *Nature* **2007**, *447*, 453–457.

(11) Wiltzius, J. J. W.; Sievers, S. A.; Sawaya, M. R.; Cascio, D.; Popov, D.; Riekel, C.; Eisenberg, D. Atomic Structure of the Cross-Beta Spine of Islet Amyloid Polypeptide (Amylin). *Protein Sci.* **2008**, *17*, 1467–1474.

(12) Liu, C.; Sawaya, M. R.; Cheng, P.-N.; Zheng, J.; Nowick, J. S.; Eisenberg, D. Characteristics of Amyloid-Related Oligomers Revealed by Crystal Structures of Macrocyclic β-Sheet Mimics. *J. Am. Chem. Soc.* **2011**, *133*, 6736–6744.

(13) Itoh, K.; Foxman, B. M.; Fasman, G. D. The Two β Forms of Poly (L-Glutamic Acid). *Biopolymers* **1976**, *15*, 419–455.

(14) Fulara, A.; Dzwolak, W. Bifurcated Hydrogen Bonds Stabilize Fibrils of poly(L-Glutamic) Acid. *J. Phys. Chem. B* **2010**, *114*, 8278–8283.

(15) Fulara, A.; Lakhani, A.; Wójcik, S.; Nieznańska, H.; Keiderling, T. A.; Dzwolak, W. Spiral Superstructures of Amyloid-like Fibrils of Polyglutamic Acid: An Infrared Absorption and Vibrational Circular Dichroism Study. *J. Phys. Chem. B* **2011**, *115*, 11010–11016.

(16) Fulara, A.; Hernik, A.; Nieznańska, H.; Dzwolak, W. Covalent Defects Restrict Supramolecular Self-Assembly of Homopolypeptides: Case Study of β_2-Fibrils of Poly-L-Glutamic Acid. *PLoS One* **2014**, *9*, e105660.

(17) Chen, S.; Ferrone, F. A.; Wetzel, R. Huntington's Disease Age-of-Onset Linked to Polyglutamine Aggregation Nucleation. *Proc. Natl. Acad. Sci. U. S. A.* **2002**, *99*, 11884–11889.

(18) Buchanan, L.; Carr, J.; Fluitt, A.; Hoganson, A.; Moran, S.; de Pablo, J.; Skinner, J.; Zanni, M. Structural Motif of Polyglutamine Amyloid Fibrils Discerned with Mixed-Isotope Infrared Spectroscopy. *Proc. Natl. Acad. Sci. U. S. A.* **2014**.

(19) Baumruk, V.; Huo, D.; Dukor, R. K.; Keiderling, T. A.; Lelievre, D.; Brack, A. Conformational Study of Sequential Lys and Leu Based Polymers and Oligomers Using Vibrational and Electronic CD Spectra. *Biopolymers* **1994**, *34*, 1115–1121.

(20) Boulmedais, F.; Schwinté, P.; Gergely, C.; Voegel, J.-C.; Schaaf, P. Secondary Structure of Polypeptide Multilayer Films: An Example of Locally Ordered Polyelectrolyte Multilayers. *Langmuir* **2002**, *18*, 4523–4525.

(21) Dzwolak, W.; Marszalek, P. E. Zipper-like Properties of [Poly(l-Lysine) + Poly(l-Glutamic Acid)] [Small Beta]-Pleated Molecular Self-Assembly. *Chem. Commun.* **2005**, 5557–5559.

(22) Dzwolak, W.; Ravindra, R.; Nicolini, C.; Jansen, R.; Winter, R. The Diastereomeric Assembly of Polylysine Is the Low-Volume Pathway for Preferential Formation of β-Sheet Aggregates. *J. Am. Chem. Soc.* **2004**, *126*, 3762–3768.

(23) Petkova, A. T.; Leapman, R. D.; Guo, Z.; Yau, W.-M.; Mattson, M. P.; Tycko, R. Self-Propagating, Molecular-Level Polymorphism in Alzheimer's Beta-Amyloid Fibrils. *Science* **2005**, *307*, 262–265.

(24) Halverson, K. J.; Sucholeiki, I.; Ashburn, T. T. Location Of. Beta.-Sheet-Forming Sequences in Amyloid Proteins by FTIR. *J. Am. Chem. Soc.* **1991**, *130*, 6701–6703.

(25) Moran, S. D.; Woys, A. M.; Buchanan, L. E.; Bixby, E.; Decatur, S. M.; Zanni, M. T. Two-Dimensional IR Spectroscopy and Segmental 13C Labeling Reveals the Domain Structure of Human γD-Crystallin Amyloid Fibrils. *Proc. Natl. Acad. Sci. U. S. A.* **2012**, *109*, 3329–3334.

(26) Holzwarth, G.; Doty, P. The Ultraviolet Circular Dichroism of Polypeptides. *J. Am. Chem. Soc.* **1965**, *87*, 218–228.

(27) Johnson, W. C.; Tinoco, I. Circular Dichroism of Polypeptide Solutions in the Vacuum Ultraviolet. *J. Am. Chem. Soc.* **1972**, *94*, 4389–4390.

(28) Clarke, D. T.; Doig, a J.; Stapley, B. J.; Jones, G. R. The Alpha-Helix Folds on the Millisecond Time Scale. *Proc. Natl. Acad. Sci. U. S. A.* **1999**, *96*, 7232–7237.

(29) Krejtschi, C.; Huang, R.; Keiderling, T. A.; Hauser, K. Time-Resolved Temperature-Jump Infrared Spectroscopy of Peptides with Well-Defined Secondary Structure: A Trpzip [Beta]-Hairpin Variant as an Example. *Vib. Spectrosc.* **2008**, *48*, 1–7.

(30) Lai, J.; Huang, Y. Fibril Aggregates of the Poly(glutamic Acid)-Drug Conjugate. *RSC Adv.* **2015**, *5*, 48856–48860.

(31) Chi, H.; Welch, W. R. W.; Kubelka, J.; Keiderling, T. A. Insight into the Packing Pattern of β2 Fibrils: A Model Study of Glutamic Acid Rich Oligomers with 13C Isotopic Edited Vibrational Spectroscopy. *Biomacromolecules* **2013**, *14*, 3880–3891.

(32) Chi, H. Spectroscopic Studies on Model Peptides of Poly-Proline in Helices and Extended Beta-Sheets, University of Illinois at Chicago, 2013.

(33) Keiderling, T. A.; Kubelka, J.; Hilario, J. Vibrational Circular Dichroism of Biopolymers. Summary of Methods and Applications. In *Vibrational spectroscopy of polymers and biological systems*; Braiman, M., Gregoriou, V. G., Eds.; CRC Press: Boca Raton, 2006; pp

253–324.

(34) Lakhani, A.; Malon, P.; Keiderling, T. A. Comparison of Vibrational Circular Dichroism Instruments: Development of a New Dispersive VCD. *Appl. Spectrosc.* **2009**, *63*, 775–785.

(35) Malon, P.; Keiderling, T. A. A Solution to the Artifact Problem in Fourier Transform Vibrational Circular Dichroism. *Appl. Spectrosc.* **1988**, *42*, 32–38.

(36) Nafie, L. A. Dual Polarization Modulation: A Real-Time, Spectral-Multiplex Separation of Circular Dichroism from Linear Birefringence Spectral Intensities. *Appl. Spectrosc.* **2000**, *54*, 1634–1645.

(37) Tanaka, S.; Scheraga, H. A. Statistical Mechanical Treatment of Protein Conformation. III. Prediction of Protein Conformation Based on a Three-State Model. *Macromolecules* **1976**, *9*, 168–182.

(38) Chi, H.; Lakhani, A.; Roy, A.; Nakaema, M.; Keiderling, T. A. Inter-Residue Coupling and Equilibrium Unfolding of PPII Helical Peptides. Vibrational Spectra Enhanced with 13C Isotopic Labeling. *J. Phys. Chem. B* **2010**, *114*, 12744–12753.

(39) Dukor, R. K.; Keiderling, T. A. Reassessment of the Random Coil Conformation: Vibrational CD Study of Proline Oligopeptides and Related Polypeptides. *Biopolymers* **1991**, *31*, 1747–1761.

(40) Zhang, G.; Babenko, V.; Dzwolak, W.; Keiderling, T. A. Dimethyl Sulfoxide Induced Destabilization and Disassembly of Various Structural Variants of Insulin Fibrils Monitored by Vibrational Circular Dichroism. *Biochemistry* **2015**, *54*, 7193–7202.

(41) Kurouski, D.; Dukor, R. K.; Lu, X.; Nafie, L. A.; Lednev, I. K. Normal and Reversed Supramolecular Chirality of Insulin Fibrils Probed by Vibrational Circular Dichroism at the Protofilament Level of Fibril Structure. *Biophys. J.* **2012**.

(42) Kurouski, D.; Dukor, R. K.; Lu, X.; Nafie, L. A.; Lednev, I. K. Spontaneous Inter-Conversion of Insulin Fibril Chirality. *Chem. Commun.* **2012**, *48*, 2837–2839.

(43) Fink, A. L. Protein Aggregation: Folding Aggregates, Inclusion Bodies and Amyloid. *Fold. Des.* **1998**, *3*, R9–R23.

(44) Sarroukh, R.; Goormaghtigh, E.; Ruysschaert, J.-M.; Raussens, V. ATR-FTIR: A

"rejuvenated" Tool to Investigate Amyloid Proteins. *Biochim. Biophys. Acta - Biomembr.* **2013**, *1828*, 2328–2338.

(45) Fabian, H.; Gast, K.; Laue, M.; Jetzschmann, K. J.; Naumann, D.; Ziegler, A.; Uchanska-Ziegler, B. IR Spectroscopic Analyses of Amyloid Fibril Formation of β2-Microglobulin Using a Simplified Procedure for Its in Vitro Generation at Neutral pH. *Biophys. Chem.* **2013**, *179*, 35–46.

(46) Gazit, E. Self Assembly of Short Aromatic Peptides into Amyloid Fibrils and Related Nanostructures. *Prion* **2007**, *1*, 32–35.

(47) Marshall, K. E.; Morris, K. L.; Charlton, D.; O'Reilly, N.; Lewis, L.; Walden, H.; Serpell, L. C. Hydrophobic, Aromatic, and Electrostatic Interactions Play a Central Role in Amyloid Fibril Formation and Stability. *Biochemistry* **2011**, *50*, 2061–2071.

(48) Adler-Abramovich, L.; Vaks, L.; Carny, O.; Trudler, D.; Magno, A.; Caflisch, A.; Frenkel, D.; Gazit, E. Phenylalanine Assembly into Toxic Fibrils Suggests Amyloid Etiology in Phenylketonuria. *Nat. Chem. Biol.* **2012**, *8*, 701–706.

(49) Evans, K. C.; Berger, E. P.; Cho, C. G.; Weisgraber, K. H.; Lansbury, P. T. Apolipoprotein E Is a Kinetic but Not a Thermodynamic Inhibitor of Amyloid Formation: Implications for the Pathogenesis and Treatment of Alzheimer Disease. *Proc. Natl. Acad. Sci.* **1995**, *92* , 763–767.

(50) Dzwolak, W.; Smirnovas, V.; Jansen, R.; Winter, R. Insulin Forms Amyloid in a Strain-Dependent Manner: An FT-IR Spectroscopic Study. *Protein Sci.* **2004**, *13*, 1927–1932.

(51) Dzwolak, W.; Jansen, R.; Smirnovas, V.; Loksztejn, A.; Porowski, S.; Winter, R. Template-Controlled Conformational Patterns of Insulin Fibrillar Self-Assembly Reflect History of Solvation of the Amyloid Nuclei. *Phys.Chem.Chem.Phys.* **2005**, *7*, 1349–1351.

(52) Hernik, A.; Puławski, W.; Fedorczyk, B.; Tymecka, D.; Misicka, A.; Filipek, S.; Dzwolak, W. Amyloidogenic Properties of Short α-L-Glutamic Acid Oligomers. *Langmuir* **2015**, *31*, 10500–10507.

(53) Kessler, J.; Keiderling, T. A.; Bour, P. Arrangement of Fibril Side Chains Studied by Molecular Dynamics and Simulated Infrared and Vibrational Circular Dichroism Spectra. *J. Phys. Chem. B* **2014**, *118*, 6937–6945.

(54) Cochran, A. G.; Skelton, N. J.; Starovasnik, M. A. Tryptophan Zippers: Stable, Monomeric β-Hairpins. *Proc. Natl. Acad. Sci.* **2001**, *98* , 5578–5583.

(55) Wu, L.; McElheny, D.; Takekiyo, T.; Keiderling, T. A. Geometry and Efficacy of Cross-Strand Trp/Trp, Trp/Tyr, and Tyr/Tyr Aromatic Interaction in a β-Hairpin Peptide. *Biochemistry* **2010**, *49*, 4705–4714.

(56) Kurouski, D.; Lombardi, R. A.; Dukor, R. K.; Lednev, I. K.; Nafie, L. A. Direct Observation and pH Control of Reversed Supramolecular Chirality in Insulin Fibrils by Vibrational Circular Dichroism. *Chem. Commun. (Camb).* **2010**, *46*, 7154–7156.

(57) Welch, W. R. W.; Kubelka, J.; Keiderling, T. A. Infrared, Vibrational Circular Dichroism, and Raman Spectral Simulations for β-Sheet Structures with Various Isotopic Labels, Interstrand, and Stacking Arrangements Using Density Functional Theory. *J. Phys. Chem. B* **2013**, *117*, 10343–10358.

(58) Mehta, A. K.; Lu, K.; Childers, W. S.; Liang, Y.; Dublin, S. N.; Dong, J.; Snyder, J. P.; Pingali, S. V.; Thiyagarajan, P.; Lynn, D. G. Facial Symmetry in Protein Self-Assembly. *J. Am. Chem. Soc.* **2008**, *130*, 9829–9835.

(59) Ni, R.; Childers, W. S.; Hardcastle, K. I.; Mehta, A. K.; Lynn, D. G. Remodeling Cross-β Nanotube Surfaces with Peptide/Lipid Chimeras. *Angew. Chemie Int. Ed.* **2012**, *51*, 6635–6638.

(60) Hauser, K.; Krejtschi, C.; Huang, R.; Wu, L.; Keiderling, T. A. Site-Specific Relaxation Kinetics of a Tryptophan Zipper Hairpin Peptide Using Temperature-Jump IR Spectroscopy and Isotopic Labeling. *J. Am. Chem. Soc.* **2008**, *130*, 2984–2992.

(61) Welch, W. R. W.; Keiderling, T. A.; Kubelka, J. Structural Analyses of Experimental 13C Edited Amide I′ IR and VCD for Peptide β-Sheet Aggregates and Fibrils Using DFT-Based Spectral Simulations. *J. Phys. Chem. B* **2013**, *117*, 10359–10369.

Figure Captions

Figure 1. A: VCD spectra of a freshly prepared $KE_{10}K$ sample. **B:** VCD spectra of this sample after high temperature incubation at 75°C. **C:** Corresponding FT-IR spectra for freshly prepared (dashed black) and incubated (red) samples.

Figure 2. VCD (**A**) and FT-IR (**B**) spectra of a $K(AE)_5K$ sample. Dashed, black traces correspond to a freshly dissolved sample and red corresponds to a sample after high temperature incubation.

Figure 3. VCD (**A**) and FT-IR (**B**) spectra of a $K(IE)_5K$ sample. Dashed, black traces correspond to a freshly dissolved sample and red corresponds to a sample after high temperature incubation.

Figure 4. A: VCD spectra of a freshly prepared sample of $K(LE)_5K$. Amide I' VCD signal initially depended on sample orientation as indicated in the various colored traces. **B:** Remeasured VCD spectra after high temperature incubation at 85°C. Orientation dependence was minimized, resulting in a qualitatively stable form having much higher intensity. **C:** Corresponding FT-IR spectra of freshly prepared (dashed, black) and incubated (red trace) samples.

Figure 5. A: VCD spectra of freshly prepared sample of $K(FE)_5K$. Amide I' VCD signal initially depended on sample orientation. **B:** Remeasured VCD spectra after high temperature incubation at 75-85°C. Orientation dependence was minimized, resulting in a qualitatively stable form having much higher intensity. The dashed regions indicate amplifier overload and therefore has approximated shape. **C:** Corresponding FT-IR spectra of freshly prepared (dashed, black) and incubated (red trace) samples.

Figure 6. TEM Images of $Lys(Phe\text{-}Glu)_5Lys$: **A.** $K(FE)_5K$ before any incubation. **B**. $K(FE)_5K$ after 75°C incubation. In expanded view, blue arrow points to wider part of the fibril and red points at the twist. Scale bars are 100 nm and 50 nm, respectively.

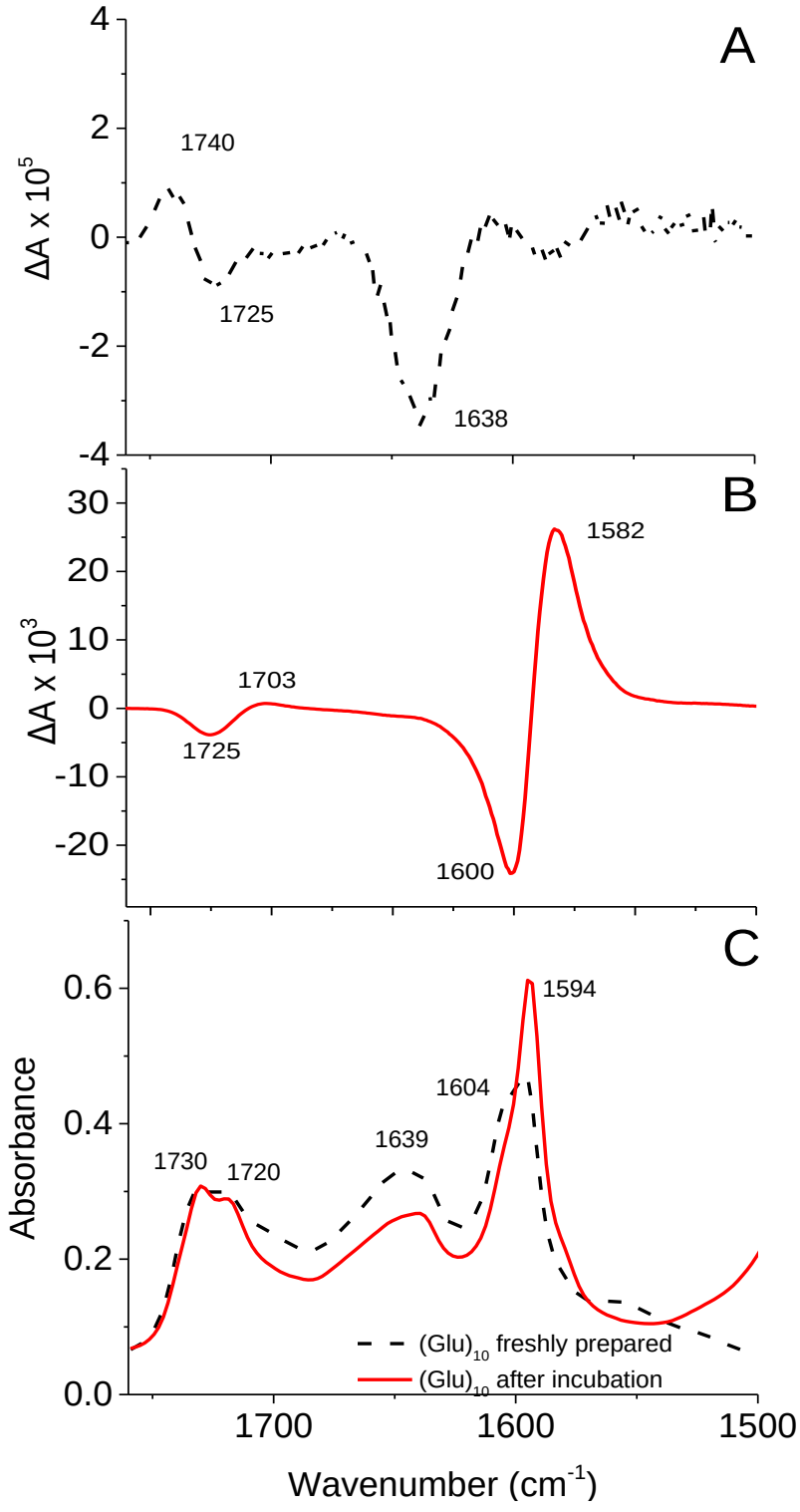

Figure 1. A: VCD spectra of freshly prepared $KE_{10}K$ sample. **B:** VCD spectra after high temperature incubation at 75°C. **C:** Corresponding FT-IR spectra for freshly prepared (dashed) and incubated (red).

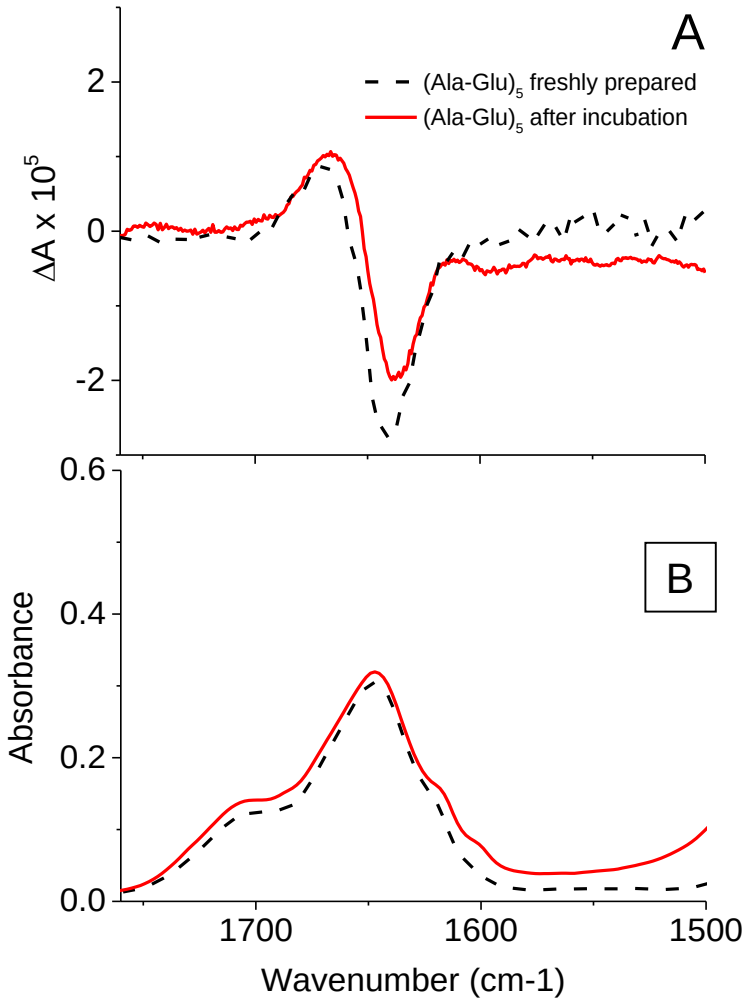

Figure 2. VCD (A) and FTIR (B) spectra of $K(AE)_5K$ sample. Dashed black traces correspond to a freshly dissolved sample and red corresponds to a sample after high temperature incubation.

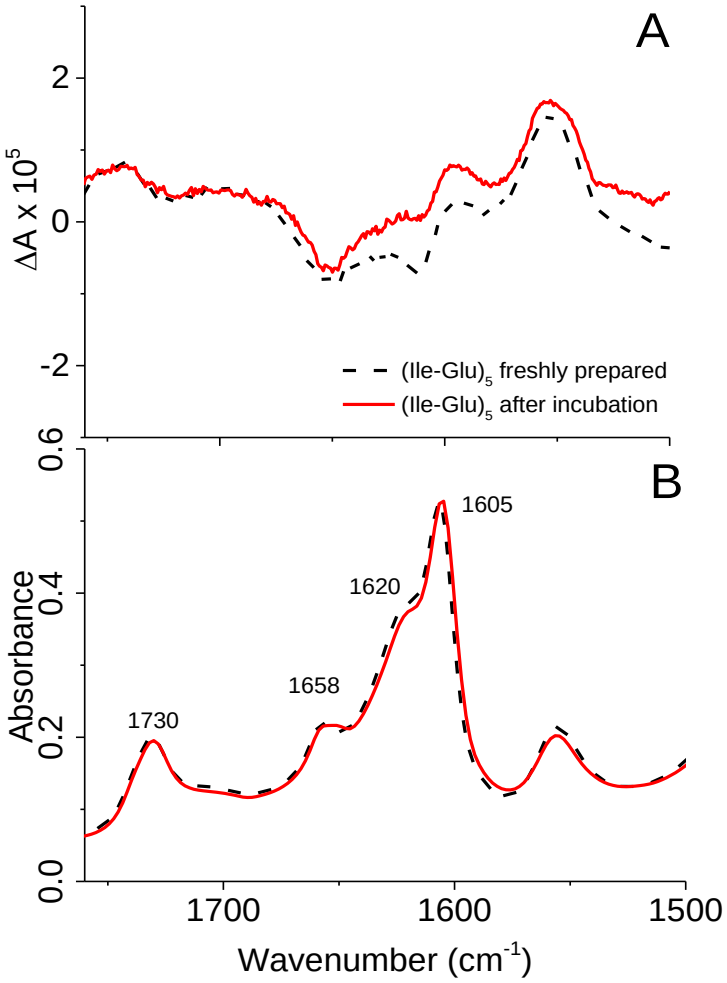

Figure 3. VCD (A) and FTIR (B) spectra of $K(IE)_5K$ sample. Dashed corresponds to a freshly dissolved sample and red corresponds to a sample after high temperature incubation.

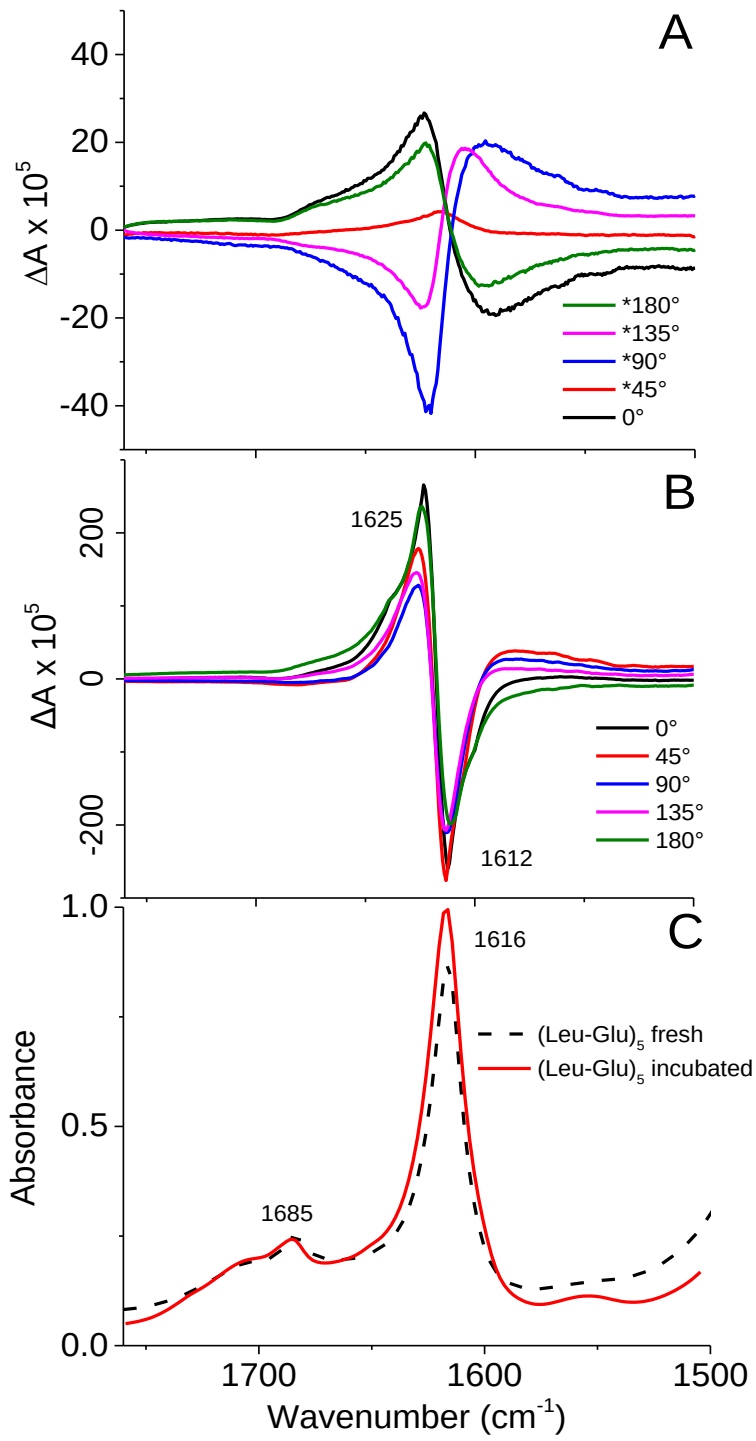

Figure 4. A: VCD spectra of the freshly prepared sample of $K(LE)_5K$. Amide I' VCD signal initially depended on sample orientation. **B:** Remeasured VCD spectra after high temperature incubation at 85°C. Orientation dependence was minimized, resulting in a qualitatively stable form of much higher intensity. **C:** Corresponding FTIR spectra of freshly prepared (dashed, black) and incubated (red trace) sample.

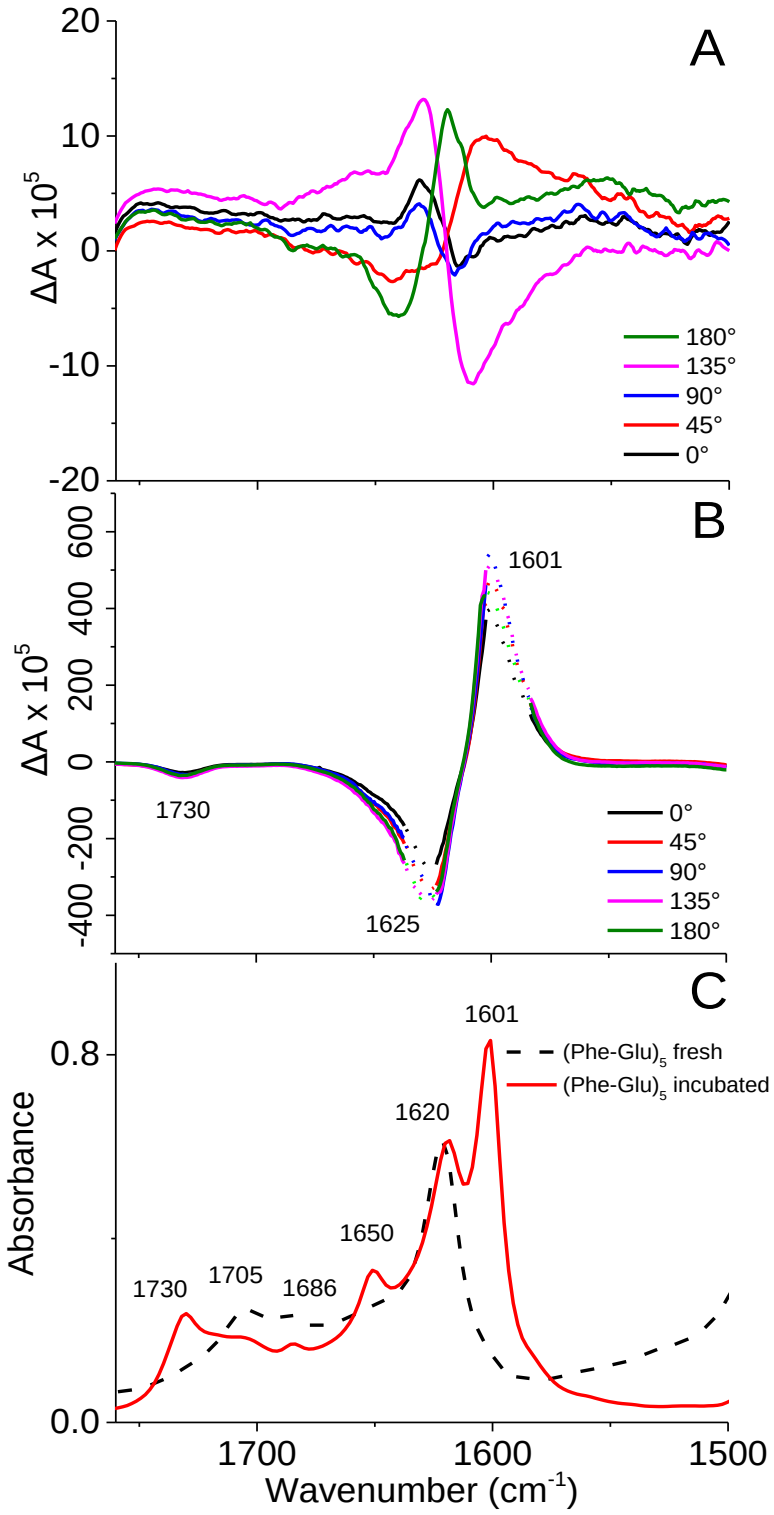

Figure 5. **A:** VCD spectra of freshly prepared sample of $K(FE)_5K$. Amide I' VCD signal initially depended on sample orientation. **B:** Remeasured VCD spectra after high temperature incubation at 75-85°C. Orientation dependence was minimized, resulting in a qualitatively stable form of much higher intensity. The dashed regions indicate amplifier overload and therefore has approximated shape. **C:** Corresponding FTIR spectra of freshly prepared (dashed, black) and incubated (red trace) sample.

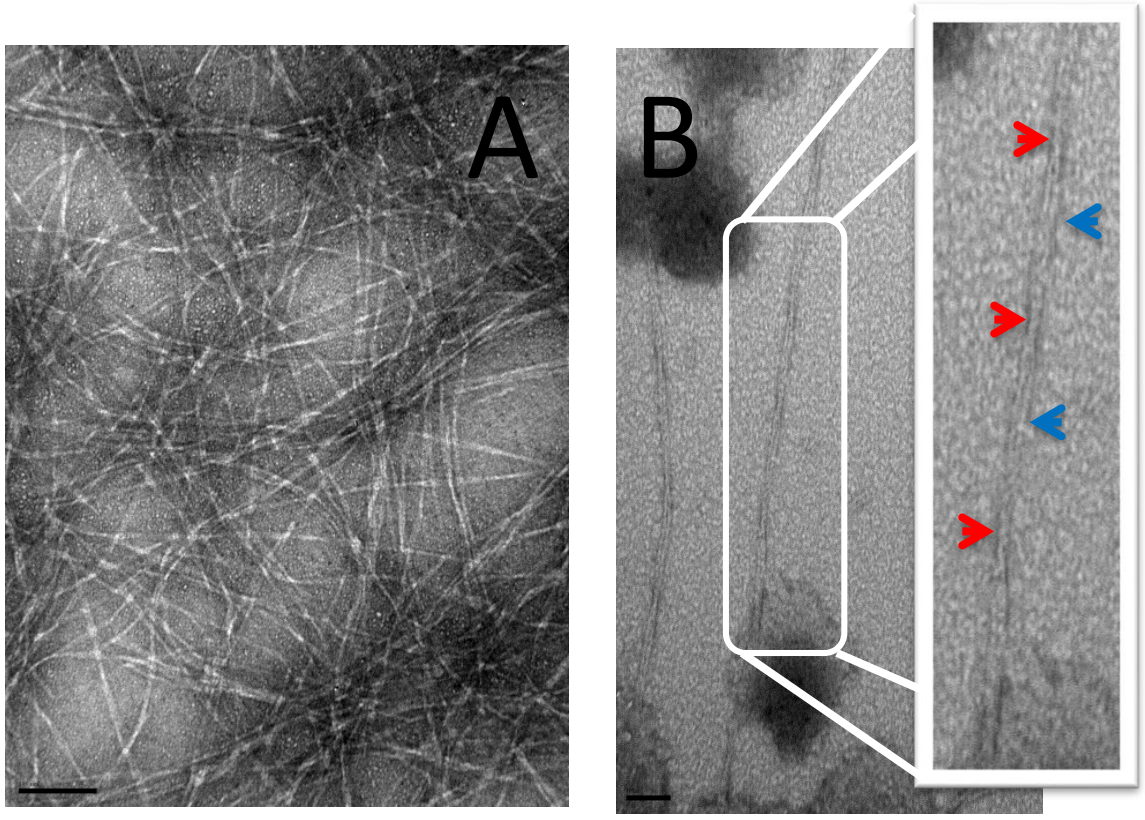

Figure 6. TEM Images of $(Phe\text{-}Glu)_5$ **A:** $K(FE)_5K_5$ before any incubation. **B**: $K(FE)_5K$ after 75°C incubation. In expanded view, blue arrow points to wider part of the fibril and red points at the twist. Scale bars are 100 nm and 50 nm, respectively.

Table of Contents graphic